Title
Generation of Pseudomonas putida KT2440 Strains with Efficient Utilization of Xylose and Galactose via Adaptive Laboratory Evolution

Journal
ACS Sustainable Chemistry & Engineering, 9(34)

ISSN
2168-0485

Authors
Lim, Hyun Gyu
Eng, Thomas
Banerjee, Deepanwita
et al.

Publication Date
2021-08-30

DOI
10.1021/acssuschemeng.1c03765

Peer reviewed

Generation of *Pseudomonas putida* KT2440 Strains with Efficient Utilization of Xylose and Galactose via Adaptive Laboratory Evolution

Hyun Gyu Lim[†,‡], Thomas Eng[‡,§], Deepanwita Banerjee[‡,§], Geovanni Alarcon[a], Andrew K. Lau[‡,§], Mee-Rye Park[‡,§], Blake A. Simmons[‡,§], Bernhard O. Palsson[†, ‡,||,#], Steven W. Singer[‡,§], Aindrila Mukhopadhyay[‡,§,††], Adam M. Feist[†,‡,||,*]

[†]Department of Bioengineering, University of California San Diego, 9500 Gilman Dr., La Jolla, CA 92093, USA

[‡]Joint BioEnergy Institute, 5885 Hollis street, 4th floor, Emeryville, CA 94608, USA

[§]Biological Systems and Engineering Division, Lawrence Berkeley National Laboratory, 1 Cyclotron Road, Berkeley, CA 94702, USA

[||]Novo Nordisk Foundation Center for Biosustainability, Technical University of Denmark, 2800 Kgs, Lyngby, Denmark

[#]Department of Pediatrics, University of California, San Diego, CA 92093, USA

[††]Environmental Genomics and Systems Biology Division, Lawrence Berkeley National Laboratory, 1 Cyclotron Road, Berkeley, CA 94702, USA

*To whom correspondence should be addressed.

(Adam M. Feist)

afeist@ucsd.edu

Abstract

While *Pseudomonas putida* KT2440 has great potential for biomass-converting processes, its inability to utilize the biomass abundant sugars xylose and galactose has limited its applications. In this study, we utilized Adaptive Laboratory Evolution (ALE) to optimize engineered KT2440 with heterologous expression of *xylD* encoding xylonate dehydratase from *Caulobacter crescentus* and *galETKM* encoding UDP-glucose 4-epimerase, galactose-1-phosphate uridylyltransferase, galactokinase, and galactose-1-epimerase from *Escherichia coli* K-12 MG1655. Poor starting strains growth (<0.1 h^{-1} or none) was evolutionarily optimized to rates of up to 0.25 h^{-1} on xylose and 0.52 h^{-1} on galactose. Whole-genome sequencing, transcriptomic analysis, and growth screens revealed significant roles of *kguT* encoding a 2-ketogluconate operon repressor and 2-ketogluconate transporter, and *gtsABCD* encoding an ATP-binding cassette (ABC) sugar transporting system in xylose and galactose growth conditions, respectively. Finally, we expressed the heterologous indigoidine production pathway in the evolved and unevolved engineered strains and successfully produced 3.2 g/L and 2.2 g/L from 10 g/L of either xylose or galactose in the evolved strains whereas the unevolved strains did not produce any detectable product. Thus, the generated KT2440 strains have the potential for broad application as optimized platform chassis to develop efficient microorganism-based biomass-utilizing bioprocesses.

Keywords: Adaptive laboratory evolution, *Pseudomonas putida*, xylose, galactose, Weimberg pathway, Leloir pathway

1. Introduction

Pseudomonas putida KT2440 (hereafter, KT2440) has been widely studied for its utilization as a microbial platform in biorefinery processes due to its tolerance to various stresses and the ability to grow on biomass-derived aromatics (e.g., coumaric acid).[1–3] Because conventional microbial hosts such as *Escherichia coli* are incapable of utilizing such aromatics, the use of KT2440 is expected to improve the cost effectiveness of bioprocesses by achieving whole-conversion of biomass-derivable carbon sources. In this regard, so far, several studies have been conducted to produce various biochemicals using KT2440.[1]

Despite these great advantages, one drawback in the use of KT2440 is that it cannot metabolize certain sugars (e.g., xylose, galactose) obtainable from biomass.[4,5] To enable xylose and galactose utilization, KT2440 has previously been engineered by the heterologous introduction of key missing genes in known sugar utilization pathways (Figure S1 and Table S1). Specifically, the xylose isomerase pathway has been constructed by the expression of xylose isomerase (XylA) and xylulokinase (XylB) from *E. coli*.[6–9] Additionally, the Weimberg pathway (i.e., xylose oxidative pathway) has been constructed by the expression of xylonate dehydratase (XylD) from *Caulobacter crescentus*.[10–12] Enabling galactose utilization has been less studied compared to xylose metabolism. Two studies reported the construction of the De Ley–Doudoroff (DLD) pathway (i.e., galactose oxidative pathway)[13] or Leloir pathway[14] by the expression of DgoKAD, galactonate catabolic enzymes, from *P. fluorescens* SBW2 or GalETKM, galactose operon, from *E. coli* K-12 MG1655, respectively.

While it was shown that KT2440 can be engineered to utilize xylose and galactose, several limitations remain. We currently have an insufficient understanding of which endogenous genes are involved in the sugar catabolism. Furthermore, initial studies have expressed heterologous

genes using plasmids, which is not ideal nor preferable for industry-scale cultivations, as plasmid-based expression increases genotypic or phenotypic instability due to its heterogeneous nature.[15,16] However, genome-based engineering often resulted in unsatisfactory cell growth (i.e., slow growth rate or long lag phase) which makes their practical deployment challenging. The successful activation of non-native sugar utilization pathways with chromosomal expression has been demonstrated for only the xylose isomerase pathway[16] and the De Ley-Doudoroff pathway.[13] Since each utilization pathway generates different intermediates and biochemical yields,[10] further studies to construct less-explored pathways in KT2440 are warranted.

In recent decades, the approach of adaptive laboratory evolution (ALE) has shown significant potential to generate useful strains for industry-relevant purposes.[17] The continuous cell culture and growth-based selection allow for the accumulation of beneficial mutations for improved fitness under a given condition. The recent development of automated ALE platforms[18,19] enabled multiplexity and controllability to change environments dynamically (e.g., substrate feeding). In addition to the strain generation, the increased accessibility to the next-generation sequencing allows for the rapid identification of genomic and transcriptomic variations in evolved cells, providing hints to understand mutational mechanisms. Indeed, many strains with industry-relevant phenotypes (e.g., higher tolerance, substrate utilization)[20–26] have been generated and their mutational mechanisms were also suggested or validated through reverse engineering. In this regard, it was expected that the ALE approach and related analysis has the potential to generate strains with improved sugar utilization and that the resulting mutational mechanisms could lead to a deeper understanding of how strains can optimize novel phenotypes related to the introduction of heterologous pathways.

In this study, an adaptive laboratory evolution (ALE) approach was applied to engineered KT2440 strains for the efficient utilization of two biomass-abundant sugars, xylose and galactose. Initially, we obtained engineered KT2440 strains (*P. putida xylD* and *P. putida galETKM,* Supplementary Data 1) in which *xylD* from *C. cresentus* or *galETKM* from *E. coli* was integrated into the chromosome to construct the Weimberg pathway for xylose utilization or the Leloir pathway for galactose utilization. Then, we evolved the strains in minimal media supplemented with xylose or galactose and we successfully obtained evolved clones that grew on xylose or galactose with higher growth rates (0.25 h^{-1} on xylose or 0.52 h^{-1} on galactose). Whole-genome and transcriptome sequencing, growth characterization of evolved isolates revealed key mechanisms that improved sugar utilization. We confirmed their capability to serve as a platform by demonstrating their efficient production of indigoidine, a naturally-found blue pigment.[27] Collectively, we expect that the generated strains and related mutational mechanisms will be greatly useful for developing KT2440-based microbial processes for the efficient production of various biochemicals from biomass.

2. Materials and Methods

Bacterial cells, plasmids, and reagents

Strains and plasmids used in this study are listed in Table S2 and S3. Plasmids were constructed by using a NEBuilder HiFi DNA assembly kit from New England Biolabs (NEB, Ipswich, MA, USA). Oligonucleotides, synthesized by Integrated DNA Technologies (IDT, Coralville, IA, USA), are listed in Table S4. The *xylD* gene was synthesized by IDT and its 5' synthetic UTR was designed by using UTR Designer.[28] For DNA amplification, Q5 High-Fidelity DNA polymerase or OneTaq DNA polymerase (NEB) was used. Plasmids were purified by using a ZymoPURE Plasmid Miniprep kit from Zymo Research (Irvine, CA, USA). Scar-less genome

engineering of the KT2440 strain was conducted as described in a previous study [22]. All chemicals were purchased from Sigma Aldrich (St. Louis, MO, USA).

Cell cultures

Cell cultures were conducted in an Luria-Bertani (LB, 10 g/L tryptone, 5 g/L yeast extract, 10 g/L NaCl) or phosphate-buffered minimal medium[22] at 30 °C. Flask-scale cell cultures were performed with a 30 mL cylindrical tube containing 15 mL of a medium. Seed cultures were prepared by inoculating colonies from LB agar plates into the minimal medium supplemented with 4 g/L glucose. Grown cultures were diluted into the fresh medium at the optical density at 600 nm (OD_{600}) of 0.1. When OD_{600} reached 0.6-1, cells were harvested and re-inoculated into xylose or galactose supplemented minimal media at OD_{600} of 0.05 to initiate main cultures. Cultures were continuously stirred at 1,100 rpm. OD_{600} was measured using a Biomate 3S bench-top spectrophotometer from Thermo Fisher Scientific (Waltham, MA, USA). For ALE, 150 μL of cultures at the late-exponential phase (OD_{600} of 0.6-1) were passaged in an automated platform.[18] During a weaning phase, 1 g/L of glucose was additionally supplemented, but its concentration was changed depending on biomass formation.[24] For a small-scale cultivation, cells were grown on a microtiter plate with a culture volume of 200 μL using an M200 Infinite Pro microplate reader from Tecan (Männedorf, Switzerland).

For the indigoidine production, cells were cultured in 250 mL baffled flasks containing 60 mL of a modified minimal medium where 2 g/L of $(NH_4)_2SO_4$ was substituted with 100 mM NH_4Cl and the sugar concentrations were increased to 10 g/L. The flasks were shaken at 200 rpm and 30 °C. Arabinose is not catabolized by KT2440 and thus 3 g/L was included to induce the expression of the indigoidine synthetic genes[14] at 0 h.

Genome and transcriptome sequencing

Genomic DNA samples were prepared by using a Quick-DNA Fungal/Bacterial Miniprep kit from Zymo Research. Sequencing library samples were prepared by using a Nextera XT kit from illumina (San Diego, CA, USA). Raw sequencing reads were obtained by using a NovaSeq 6000 (illumina) at the UC San Diego IGM Genomics Center and analyzed by using Breseq (version 0.33.1)[29] and Bowtie2 (version 2.3.4.1).[30] Analysis results were uploaded to ALEdb v1.0.[31]

RNA samples were prepared from cells at the exponential phase (OD_{600} 0.4-0.6) using an RNAprotect Bacteria Reagent from Qiagen and a Quick-RNA Fungal/Bacterial Miniprep kit from Zymo Research. Ribosomal RNA was removed as described in a previous study.[22] Paired-end libraries were prepared by using a KAPA RNA HyperPrep kit from Kapa Biosystems (Wilmington, MA, USA) and sequenced using the NovaSeq 6000. Raw sequencing files were processed using Bowtie2[30] and summarizeOverlaps.[32] Differentially expressed genes were detected by using DEseq2.[33]

Biomass and metabolite quantification

Cell biomass was determined by converting OD_{600} to a dry cell weight (DCW)/L using a conversion factor of 0.38.[8] Metabolite concentrations were quantified by using a 1260 Infinity II LC system (Agilent, Santa Clara, CA, USA) equipped with an HPX-87H (Biorad, Hercules, CA, USA) and a refractive index detector. 5 mM H_2SO_4 was used as a mobile phase at a flow rate of 0.5 mL/min. The column temperature was maintained at 45 ^{o}C.

Indigoidine was quantified after its extraction using dimethyl sulfoxide as described in a previous study.[14,34] The absorbance at 612 nm was measured by using a microtiter plate reader from BD Biosciences (Molecular Devices, CA, USA). The theoretical maximum yield from xylose was calculated as 0.74 g indigoidine/g xylose using the modified KT2440 metabolic model

iJN1462[3] to account for xylose utilization through the Weimberg pathway. The yield from galactose (0.77 g indigoidine/g galactose) was adapted from a previous study.[14]

Protein structure prediction and visualization

Protein structures were predicted by using the I-TASSER software [35]. Predicted structures were visualized by using the UCSF Chimera.[36]

3. Results

Adaptive laboratory evolution of engineered *P. putida* strains for xylose and galactose utilization enhances catalytic capabilities

The initial growth characteristics of two engineered KT2440 strains (*P. putida xylD* and *P. putida galETKM*) in minimal media supplemented with either xylose or galactose as a sole carbon source were characterized. In the *P. putida xylD* strain, only the *xylD* gene from *C. crescentus* was introduced to construct the Weimberg pathway for xylose utilization because it was shown that the conversion of xylose to xylonate can be mediated by the native glucose dehydrogenase (encoded by *gcd*, PP_1444) (Figure S1).[11] *xylD* was expressed from the chromosome under a constitutive promoter and 5'-untranslated region (Supplementary Note 1). Consistent with previous observations,[11] the expression of *xylD* enabled growth of the strain on xylose as a sole carbon source (Figure S2A); however, it showed a relatively low growth rate (μ, ~ 0.07 h^{-1}), long lag time (> 36 h), and clumping (data not shown) during initial growth characterizations. For the second starting strain, we utilized a previously constructed *P. putida galETKM* strain [14], in which the native galactose operon (*galETKM*) of *E. coli* K-12 MG1655 was introduced into the chromosome

to construct the Leloir pathway. This *P. putida galETKM* starting strain did not display observable growth on galactose minimal medium during a 48 h culture screen (Figure S2B); the strain did grow under a rich medium or glucose minimal medium condition. These initial screens set the starting parameters for a multifaceted ALE strategy to improve the sugar utilization of both KT2440 strains on their respective sole carbon source sugars.

ALE experiments with two different strategies were conducted to optimize growth rates and catalytic activity on the targeted xylose and galactose sugars. Given that the *P. putida xylD* strain could initially grow on xylose, we continuously propagated the strain in a constant condition ALE on an automated platform[37] on minimal medium supplemented with xylose (4 g/L) as the sole carbon source (Figure 1A). For the *P. putida galETKM* starting strain, which could not initially grow solely on galactose within 48 h, we propagated the strain in a minimal medium containing 4 g/L galactose and the additional supplement of 1 g/L glucose to support cell growth and subsequent mutation accumulation (Figure 1B); this complementary approach was also automated and adapted from Guzman et al[24]. The supplemented culture (hereafter referred to as the main culture) was regularly screened by inoculating it into a fresh galactose-only minimal medium (hereafter referred to as the test culture). If cells failed to produce an observable grow rate during 48 h in the test culture, it was discarded, and the main culture was continued. Once a stable growth rate ($\mu > 0.05$ h^{-1}) in a test culture was observed for a given replicate after several generations, this culture was continued as a constant condition galactose-only culture and continued for growth rate selection until the end of the experiments. It should be noted that in the original main culture line, the amount of glucose was gradually decreased, depending on the final biomass density during stationary phase, as previously described.[24] Both strategies of automated ALE experiments were parallelly conducted with four independent biological replicates (Table S5).

The ALE experiments were conducted for approximately three months (203-479 generations, equivalent to 11.5-30.5 × 10^{11} cumulative cell divisions). Notably, the growth rates of all independent replicates of *P. putida xylD* populations were significantly increased at an early stage of the experiments (ALE1-4 and Figure 1C). However, no further significant increases were observed; the final growth rates of populations were between 0.22 and 0.25 h^{-1}. In the case of the *P. putida galETKM* strain (Figure 1D), successful growth on solely galactose was observed in three replicates (ALE5, ALE6, and ALE8). The passage numbers before displaying the stable growth varied between 35 – 44 flasks (Table S5). Although the initial growth rates of these novel populations were relatively low (approximately 0.1 h^{-1}), the rates were gradually increased over time and reached between 0.33 h^{-1} and 0.52 h^{-1}, indicating that the evolved strains acquired beneficial mutations which improved galactose catabolism.

Clones were isolated from each experiment at several time points and validated to display the observed phenotypes from the evolved populations. Two or three intermediate evolutionary time points for ALE 1 - 4 and four points for ALE 5, 6, 8 (Figure 1C and 1D) were isolated and their specific growth rates during exponential growth were measured in the xylose or galactose minimal medium, respectively (Figure 1E and 1F). For clones derived from the *xylD* starting strain, the growth rates of isolates generally corresponded to the growth rates of populations from which the strains were isolated; they were in a range of 0.20 h^{-1} - 0.26 h^{-1}, regardless of isolation timepoints. Conversely, the growth rates of evolved *P. putida galETKM* clones from later evolutionary time populations were greater than those isolated from early populations; the end-point isolates showed the growth rates between 0.35 h^{-1} and 0.52 h^{-1}.

Growth, sugar consumption, and biomass yields were determined in detail to physiologically characterize evolved strains and compare them to the starting strains (Figure 2).

The earliest isolated *P. putida xylD* clones (A1_F11_I1, A2_F10_I1, A3_F14_I1, and A4_F11_I1) from first-time points and the end-point *P. putida galETKM* clones (A5_F85_I1, A6_F90_I1, and A8_F92_I1) were selected as representative clones for in depth physiological characterization. While the starting strains showed no growth with the consumption of a negligible or small amount of xylose or galactose, the evolved strain demonstrated greatly improved growth and sugar consumption. The four evolved *P. putida xylD* clones showed similar growth and sugar consumption profiles (Figure 2A and 2B). Among them, their xylose uptake rates varied by 1.6-fold (Figure 2A-C); the A1_F11_I1 strain showed the highest uptake catalytic rate (1.2 g xylose g DCW^{-1} h^{-1}), but the lowest biomass yield (0.20 g xylose g DCW^{-1}). Interestingly, the three isolated evolved *P. putida galETKM* clones showed noticeably different growth and sugar consumption profiles (Figure 2D-F). Only the A6_F90_I1 strain fully grew and consumed the provided 4 g/L galactose in 24 h of culturing at the lowest uptake rate of 1.3 g galactose g DCW^{-1} h^{-1} of all isolated clones. While the sugar uptake rates of the other *P. putida galETKM* clones were 1.3- and 2.0-fold higher, these two strains did not fully consume galactose and growth ceased after reaching OD_{600} of 0.85 or 1.2, resulting in two- or three-times less final biomass density and yield. Additionally, the growth rates of all the characterized clones on glucose remained at similar levels compared to the wild-type strain (Figure S3). While there are several differences, all isolates showed significantly improved sugar (i.e., xylose and galactose) consumption capabilities when compared to the starting strains, confirming that the ALE strategy was successful in generating strains with enhanced catalytic activity for both xylose and galactose utilization.

Genomic and transcriptomic sequencing elucidates causal mutations and their impact on enhanced catalytic phenotypes

To identify beneficial mutations in the engineered and evolved strains on xylose and galactose, we conducted whole-genome sequencing of clones isolated during the middle (i.e., intermediate) and end of the evolutions (i.e., endpoints). Furthermore, the transcriptomes of a set of selected clones were measured and analyzed to understand the effect of mutations and resulting transcriptional changes in the different carbon source culturing environments.

3.2.1. Whole-genome sequencing revealed mutations on transport and catabolic processes

Whole genome sequencing of eleven *P. putida xylD* and twelve *P. putida galETKM* evolved isolates successfully revealed several genes or regions (hereafter, collectively referred to as regions) commonly mutated across the independently evolved replicates (Supplementary Information, Figure 3A and 3B). Surprisingly, mutations in six (*ptxS*, *kguT*, *gacS*, *ftsH*, PP_4173, and *galP*-I/PP_1174) and three (*gtsABCD*, *oprB*-I/*yeaD*, and *oprB*-II) regions accounted for 44% (38 out of 86) and 32% (20 out of 63) of the total mutations in *P. putida xylD* and *P. putida galETKM* isolates, respectively (Table 1). Although we expected frequent mutations in the heterologous genes, given that heterologous gene expression cassettes have been mutation targets in previous heterologous pathway optimization studies,[16,38] only the *galETKM* region was mutated in isolates from ALE 8 where a single amino acid change mutation in *galK* and single nucleotide change in the intergenic region between *galE* and its neighboring gene, *prfC* were observed; no mutations occurred in the *xylD* region. Furthermore, it should be noted that the A4_F56_I1 and A6_F90_I1 clones acquired mutations in *mutS*, encoding a mismatched DNA repair protein.[39] In particular, a relatively higher number of mutations (42 mutations) were identified in the former strain when compared to mutation numbers of other isolates (up to 10 mutations).

The two genes responsible for one of three peripheral glucose utilization pathways (*ptxS* and *kguT*, Figure 3C), were highly mutated in all eleven sequenced *P. putida xylD* isolates (100% for *ptxS* and 82% for *kguT*) suggesting their critical roles for the improved xylose utilization (Figure 3A). It is known that *ptxS* encodes a LacI-family transcription factor, namely a 2-ketogluconate utilization repressor. The binding of 2-ketogluconate mediates the dissociation of PtxS from the promoter region of the *kguEKT-ptxD* operon.[40–42] Since the mutations which altered the DNA binding motif (R30S, S29F, or V28F) and partial deletions (Δ51 or Δ438 bp) of PtxS were identified in the isolates, it implies that these mutations de-repressed the expression of *kguE*, *kguK*, *kguT*, and *ptxD* and as a result, enabled an increase in xylose catabolism. Mutations found in KguT were mostly SNPs (seven unique SNPs found overall) which effected changes in single amino acids, a small deletion, or changes in a few amino acids at the end of the protein (Figure S4A), likely effecting the transportation of xylonate. Interestingly, it was found that the A2_F10_I1 and A3_F14_I1 strains with relatively lower xylose uptake rates (Figure 2C) did not acquire any mutations in KguT. Thus, an association can be drawn between major xylose catabolic and growth rate improvements and mutations in *ptxS* and *kguT* simultaneously in the strains examined.

Additional genetic regions were independently mutated in two or more *xylD* ALE experiments (Table 1), in addition to the *ptxS* and *kguT* regions, at a lower frequency. These regions were *gacS* (36%), *ftsH* (27%), PP_4173 (27%), and *galP*-I/PP_1174 (the intergenic region between *galP*-1 and PP_1174, 18%). Mutations in *gacS* (encoding a sensor protein, GacS) and PP_4173 (encoding a two-component system sensor histidine kinase/response regulator) were also found in previous ALE studies examining tolerance to different compounds, but with a similar base media and growth environment.[21,22] Thus, the *gacS* and PP_4173 mutations appear to be

related to general adaptation to the media or culturing environment used in this study. However, the mutations in *ftsH* (encoding an Integral membrane ATP-dependent zinc metallopeptidase) and *galP*-I (encoding a porin-like protein)/PP_1174 (encoding a hypothetical protein) have not been previously identified in an ALE study and it is unclear how they relate to the specific xylose utilization phenotype.

In the case of evolved *P. putida galETKM* isolates, the three commonly mutated regions were related to the transport of glucose (Table 1), implying galactose transportation was the major bottleneck. Most importantly, mutations in the *gtsABCD* region were observed in all three endpoint isolates as well as many intermediate isolates (66%, Figure 3B). Clear growth rate increases were observed after acquiring one of these mutations (F2 → F21 in ALE5, F13 → F39 in ALE6, F1 → F38 in ALE8, Figure 1E and 1F). These genes encode an ATP-binding cassette (ABC) sugar transporting system, consisting of a sugar-binding protein (GtsA), two subunits of an ABC transporter (GtsB and GtsC), and an ATP binding protein (GtsD); this system is known to transport glucose into the cytosol through the inner membrane.[40] All endpoint clones acquired mutations in *gtsA* (A100V, N304D, N304S, and A427V) and mutations in *gtsC* (F122L, L133F, and T238I) were observed only in clones from ALE8 (Figure S4B and S4C). Previously, it was observed that mutations in *gtsABCD* allowed the transportation of xylose,[43] indicating its promiscuity in transporting other compounds. Similarly, these frequent mutations in the *gtsABCD* region strongly suggested that the major bottleneck was the transportation of galactose into the cytosol. In addition to *gtsABCD*, two other regions related to glucose metabolism (*oprB*-I/*yeaD* and *oprB*-II) were also commonly mutated (Figure 3B). OprB porins are known to transport glucose into the periplasm.[40,44] Mutations in *oprB*-I (encoding carbohydrate-selective porin-I)/*yeaD* (encoding glucose-6-phosphate 1-epimerase) regions were a stop codon insertion and frameshift in *oprB*-I,

or single nucleotide mutation in their intergenic region. Given that two *oprB*-I mutations are loss of function mutations, it was inferred that its mutation was not beneficial for galactose utilization. In *oprB*-II, a silent mutation (Y265Y) identically occurred in two endpoint isolates from ALE5 and ALE8 (Figure 3B) which displayed relatively higher galactose consumption rates compared to the endpoint isolate from ALE6 (Figure 2F). The same mutation was also observed in previous evolution studies with glucose,[21,22] suggesting that it likely improves the transport of hexoses into the cytosol.

3.2.2 Transcriptome analysis of evolved clones confirms the xylose and galactose utilization pathways

Transcriptomes of representative clones grown on xylose or galactose were analyzed to better understand how these sugars are utilized via RNA-Seq. We focused on the expression level changes of mutated genes and other endogenous genes in central carbon metabolism (Figure 3C) and compared with the transcriptome of the wildtype KT2440 strain growing on glucose[22] as a reference. In the four evolved *P. putida xylD* isolates analyzed, the expression levels of *ptxS*, *kguETK,* and *ptxD* genes were indeed highly up-regulated, likely due to the derepression by PtxS (Figure 3D). Specifically, the expression level of *kguT* was increased by 20.3-fold, on average, when compared to that of the wildtype grown on glucose. Although a previous study suggested that *gntT* is responsible for the transportation of xylonate,[11] its expression level was greatly decreased, suggesting that xylonate is transported by KguT, and not GntT. Additionally, it was observed that the expression levels of the PP_2834-2837 genes were significantly increased (fold changes > 500). One of these genes, PP_2836, was previously suggested to encode 2-keto-3-deoxy-xylonate dehydratase.[10,11] The upregulation of PP_2836 supports the hypothesis on its role

to enable xylose metabolism via the Weimberg pathway. In addition to up-regulated genes, there were also noteworthy down-regulated genes; given that xylose directly enters the TCA cycle after its conversion to α-ketoglutarate, genes related to glucose metabolism were relatively down-regulated.

The expression levels in the three evolved *P. putida galETKM* strains were also investigated to confirm the galactose utilization pathway and to investigate transcriptional changes of three mutated regions (*gtsABCD*, *oprB*-I/*yeaD*, and *oprB*-II, Figure 3D). As expected, the expression levels of *gtsABCD* were highly up-regulated (up to 9-fold) in the three isolates (Figure 3D), showing that they are closely related to the improved galactose utilization. The expression levels of *oprB*-I, in which perceived loss-of-function mutations occurred, were commonly increased (5.3-fold on average) while the *yeaD* expression levels changed inconsistently at lesser extents. Notably, the expression levels of *oprB*-II were indeed increased in the two endpoint isolates with the Y265Y mutation in this gene (the A5_F85_I1 and A8_F92_I1 strains) by 13.8-fold and 9.7-fold, respectively (Figure 3B), whereas the level in the A6_F90_I1 without the mutation decreased by 5.0-fold. This observation supports that this synonymous mutation, upregulates its expression; previously, changed gene expression levels by synonymous mutations have been observed in *Pseudomonas* species.[45] Furthermore, it was likely that this mutation also affected the expression of a downstream gene, *gcd*, as its levels were similarly changed (5.6-fold and 6.8-fold increases in the two strains with the mutation and a 3.7-fold decrease in the other strain). The effect of *gcd* was further evaluated in a targeted analysis (see below). Additionally, we compared the expression levels of the *galETKM* genes and their neighboring PP_0871 and *prfC* genes (Figure S6) to investigate potential transcriptional changes caused by the two mutations in the A8_F92_I1 stain (Supplementary Data 3). However, the levels in the A8_F92_I1 strain were

generally similar to those in A5_F85_I1, which do not have any mutations in this region, indicating that they do not significantly affect the transcription levels.

Reverse engineering validates the xylose and galactose utilization pathways and phenotypes

The essentiality of the heterologous and mutated genes was examined via gene deletions and subsequent growth measurements on the constructed clones. Initially, the heterologous *xylD* or *galETKM* gene was deleted in the A1_F11_I1 strain and A6_F90_I1 strain, respectively. Unsurprisingly, the A1_F11_I1_Δ*xylD and* A6_F90_I1_Δ*galETKM* strains completely lost their capability to grow on xylose or galactose (Figure 4A and 4B), respectively, confirming the essentiality of these genes. It is worthwhile to note that despite the presence of an endogenous *fucD* encoding fuconate dehydratase (which was significantly overexpressed by on average 62.6-fold, Figure 3D), this potential promiscuous activity could not support xylose-based growth in the strain. Next, we validated the roles of two frequently mutated genes (*kguT* and *gtsABCD*). As expected, the A1_F11_I1_Δ*kguT and* A6_F90_I1_Δ*gtsABCD* strains lacking the mutated transporter could not grow on xylose or galactose, respectively, confirming that these sugar transporters are indeed critical to the sugar metabolism. Collectively, these results indicate that xylose and galactose are utilized via the introduced Weimberg and Leloir pathways, respectively, and KguT and GtsABCD are essential for their respective sugar metabolism.

The effect and removal of *gcd* was evaluated in evolved strains given its significant upregulation and its known role in generating growth-inhibiting dead-end byproducts due to its broad substrate specificity.[8,12,46] Clones A5_F85_I1 and A8_F92_I1 were evaluated using a deletion of *gcd* for this analysis as their growth was arrested before full galactose consumption during phenotypic characterization (Figure 2E). Indeed, after the deletion of *gcd*, the two strains

(A5_F85_I1_Δ*gcd* and A8_F92_I1_Δ*gcd*) showed significantly increased biomass formation and galactose consumption (Figure 4C). The final OD_{600} reached 2.69 and 2.67 and 4 g/L galactose was fully consumed during 24 h, respectively. Galactose uptake rates were 0.85 g/g DCW/h and 1.61 g/g DCW/h, respectively, which is a slight reduction versus their parent strains over the same time window. Overall, these results confirmed that *gcd* overexpression induced stunted growth of the two evolved isolates and this phenomenon was not observed in clone A6_F90_I1, which did not possess a mutation in the neighboring *oprB*-II.

Production of indigoidine with the evolved isolates

The applicability of the evolved strains and further *gcd*-deleted strains as preferred host chassis for the biochemical production of indigoidine from either xylose or galactose was examined. In particular, the Δ*gcd* strains were included, given that the deletion did not significantly affect the growth rates on glucose (Figure S3). For this demonstration, we introduced the production pathway of indigoidine, which is a natural pigment and has industrial interest,[14,47,48] in evolved isolates (Figure 5A). It was previously shown that indigoidine can be produced by the heterologous expression of *bpsA* encoding blue pigment synthetase A from *Streptomyces lavendulae* and *sfp* encoding 4′-phosphopantetheinyl transferase from *Bacillus subtilis*.[14,47] We expressed the two genes under the arabinose-inducible promoter and integrated them into the genome (see Methods). Subsequently, the resulting strains were cultivated in minimal media supplemented with 10 g/L xylose or galactose. The cultivation showed that all evolved strains with the heterologous production pathway successfully produced indigoidine, whereas the starting strain with the pathway did not produce a detectable amount of indigoidine (Figure 5B and Figure S7). The titers varied, on average 2.5 ± 0.8 g/L for xylose and 0.8 ± 0.5 g/L for galactose at 48 h,

depending on the sugar source and host, indicating that the use of different sugars and host genotypes significantly affect the production. Specifically, xylose utilization via the Weimberg pathway allowed much higher indigoidine titers (3.1-fold on average) compared to the galactose utilization via the Leloir pathway. Among them, the A2_F10_I1_indigoidine strain produced 3.2 g/L, which is a higher value than the titer (1.5 - 2 g/L) from the same amount of glucose.[14] The titer of 2.2 g/L achieved by the A6_F90_I1 strain was also comparable, while the other two strains did not show high titers, probably due to the stalled growth and galactose consumption (Figure 4). Both Δ*gcd* strains showed improved indigoidine production compared to their parental strains, but the titers were still less than that achieved with the A6_F90_I1 strain. The highest titers for each carbon source represent up to 43% and 29% of the maximum theoretical production (see Methods for calculation). Collectively, this successful demonstration of the indigoidine production supports the applicability of the evolved clones in various biochemical production processes as optimized chassis when compared to the initial engineered, but unevolved counterparts.

4. Discussion

To develop economically feasible bioprocesses, it is essential to utilize host microorganisms that efficiently utilize carbon sources available from biomass.[49–51] However, often the catabolic activities of wildtype microorganisms are not high enough, and require further engineering. While there are many successful studies showing that rationally engineered microorganisms improve the utilization of native or non-native carbon sources,[4,52–54] an initial design could fail or result in unsatisfactory utilization due to the inability to precisely engineer a microorganism. In this regard, our study demonstrated that an ALE strategy can complement a rational strain design strategy and generate improved strains by efficiently seeking beneficial

mutations from a large sequence space. Additionally, we showed that ALE allows for a deeper understanding of host microorganisms by performing multi-scale analyses of evolved and reverse engineered strains. The genome and transcriptome sequencing of independently evolved clones were crucial to understand how xylose and galactose are catabolized and to identify rate-limiting steps in KT2440. In addition, the analysis was also important to understand the range of phenotypes possible in evolved clones and was utilized to further engineer the strains.

Interestingly, the final growth rates of *P. putida xylD* evolved clones on xylose (0.23-0.25 h^{-1}) were relatively slower than those of *P. putida galETKM* on galactose (0.35-0.52 h^{-1}). Similarly, different endpoint growth rates depending on sugars were also observed in a previous ALE study with *E. coli* K-12 MG1655.[55] Potentially, the xylose oxidation activity of Gcd could be another rate-limiting step given xylose is likely not a native substrate.[56,57] Although it is not currently clear why the growth rates on xylose remained at low levels and were not further improved, considering that typical biomass hydrolysates contain multiple sugars, the *P. putida xylD* clones could consume other sugars (e.g., glucose, Figure S3) and show higher growth rates during fermentation with actual biomass-derived feedstocks. If even higher growth rates are desired, further ALE experiments with increased mutation rates or combining multiple catabolic pathways could be performed. Growth rates on glucose greater than 0.8 h^{-1} have been observed in previous ALE studies.[21,22] Finally, the finding that similar growth rates of the evolved clones to the wild type on glucose (Figure S3) indicates that the evolved strains are not entirely specialized and the mutations they possess appear to be local to the targeted sugar uptake pathways.

Additionally, more value can be added if the simultaneous utilization of multiple sugars is studied and ALE can similarly aid in the optimization of such strains. A bioprocess for the simultaneous utilization can be directly designed by co-culturing the generated strains for the

specified utilization of sugars.[58,59] More promisingly, separately evolved and optimized pathways and mutations could be introduced into a single strain and inherent preferential utilization mechanisms can be deregulated. Previously, the deletion of carbon catabolite repression protein (Crc) was shown to enable the simultaneous utilization of sugars and aromatics.[16] Alternatively, one can also apply another ALE strategy that grows a strain under a substrate-switching condition or mixed-substrate condition[55,60] to facilitate the utilization of multiple sugars. These efforts have the potentially to greatly improve titers, productivities, and yields by increasing the substrate consumption rate (i.e., front end engineering), which are critical measures in bioprocess.

In summary, we successfully generated *P. putida* KT2440 strains for the efficient utilization of xylose and galactose. The ALE approach successfully overcomes the limitation of rational strain design and enabled significantly improved xylose and galactose utilization capabilities. Furthermore, our indigoidine production results show the strong potential of the developed strains to improve the economic viability. We believe the developed strains as well as mutational mechanisms could be useful for developing efficient biomass-converting processes.

Acknowledgements

This work conducted by the Joint BioEnergy Institute was supported by the Office of Science, Office of Biological and Environmental Research, of the U.S. Department of Energy under Contract No. DE-AC02-05CH11231. We would like to appreciate Dr. José Henrique Pereira, Joshua Mueller, and Patrick V. Phaneuf for helpful discussion. We also thank Connor A. Olson, Richard Szubin, Ying Hutchison, and Marc K. Abrams for technical support and manuscript editing.

Conflict of Interest

Hyun Gyu Lim, Adam M. Feist, and Thomas Eng are the inventors of U.S. Provisional Application Serial No. 63/168,687 based on this study. The other authors declare no competing financial interest.

Supporting Information

Figure S1. Pathways for glucose, xylose, and galactose utilization

Figure S2. Growth profiles of the wildtype KT2440 and engineered strains on xylose and galactose

Figure S3. Growth rate comparison of the wildtype KT2440 and evolved strains on glucose

Figure S4. I-TASSER predicted structures of KguT, GtsA, and GtsC and their mutations

Figure S5. Cluster of orthologous groups (COG) analysis of commonly differentially expressed genes

Figure S6. Transcripts per million of the *galETKM* genes and their neighboring genes

Figure S7. Standard curve for indigoidine quantification

Table S1. Previous studies for enabling non-native sugars in *P. putida* strains

Table S2. Stains used in this study

Table S3. Plasmids used in this study

Table S4. Oligonucleotides used in this study

Table S5. Summary of the ALE experiments

References

(1) Nikel, P. I.; de Lorenzo, V. *Pseudomonas putida* as a functional chassis for industrial biocatalysis: From native biochemistry to trans-metabolism. *Metab. Eng.* **2018**, *50*, 142–155.

(2) Belda, E.; van Heck, R. G. A.; José Lopez-Sanchez, M.; Cruveiller, S.; Barbe, V.; Fraser, C.; Klenk, H.-P.; Petersen, J.; Morgat, A.; Nikel, P. I.; et al. The revisited genome of Pseudomonas putida KT2440 enlightens its value as a robust metabolic chassis. *Environ. Microbiol.* **2016**, *18*, 3403–3424.

(3) Nogales, J.; Mueller, J.; Gudmundsson, S.; Canalejo, F. J.; Duque, E.; Monk, J.; Feist, A. M.; Ramos, J. L.; Niu, W.; Palsson, B. O. High-quality genome-scale metabolic modelling of *Pseudomonas putida* highlights its broad metabolic capabilities. *Environ. Microbiol.* **2020**, *22*, 255–269.

(4) Lim, H. G.; Seo, S. W.; Jung, G. Y. Engineered Escherichia coli for simultaneous utilization of galactose and glucose. *Bioresour. Technol.* **2013**, *135*, 564–567.

(5) Isikgor, F. H.; Becer, C. R. Lignocellulosic biomass: a sustainable platform for the production of bio-based chemicals and polymers. *Polym. Chem.* **2015**, *6*, 4497–4559.

(6) Meijnen, J.-P.; de Winde, J. H.; Ruijssenaars, H. J. Engineering Pseudomonas putida S12 for efficient utilization of D-xylose and L-arabinose. *Appl. Environ. Microbiol.* **2008**, *74*, 5031–5037.

(7) Le Meur, S.; Zinn, M.; Egli, T.; Thöny-Meyer, L.; Ren, Q. Production of medium-chain-length polyhydroxyalkanoates by sequential feeding of xylose and octanoic acid in engineered Pseudomonas putida KT2440. *BMC Biotechnol.* **2012**, *12*, 53.

(8) Dvořák, P.; de Lorenzo, V. Refactoring the upper sugar metabolism of Pseudomonas putida for co-utilization of cellobiose, xylose, and glucose. *Metab. Eng.* **2018**, *48*, 94–108.

(9) Wang, Y.; Horlamus, F.; Henkel, M.; Kovacic, F.; Schläfle, S.; Hausmann, R.; Wittgens, A.; Rosenau, F. Growth of engineered*Pseudomonas putida* KT2440 on glucose, xylose and arabinose: hemicellulose hydrolysates and their major sugars as sustainable carbon sources. *Glob. Change Biol. Bioenergy* **2019**.

(10) Bator, I.; Wittgens, A.; Rosenau, F.; Tiso, T.; Blank, L. M. Comparison of Three Xylose Pathways in *Pseudomonas putida* KT2440 for the Synthesis of Valuable Products. *Front. Bioeng. Biotechnol.* **2019**, *7*, 480.

(11) Meijnen, J.-P.; de Winde, J. H.; Ruijssenaars, H. J. Establishment of oxidative D-xylose metabolism in Pseudomonas putida S12. *Appl. Environ. Microbiol.* **2009**, *75*, 2784–2791.

(12) Shen, L.; Kohlhaas, M.; Enoki, J.; Meier, R.; Schönenberger, B.; Wohlgemuth, R.; Kourist, R.; Niemeyer, F.; van Niekerk, D.; Bräsen, C.; et al. A combined experimental and modelling approach for the Weimberg pathway optimisation. *Nat. Commun.* **2020**, *11*, 1098.

(13) Peabody, G. L.; Elmore, J. R.; Martinez-Baird, J.; Guss, A. M. Engineered Pseudomonas putida KT2440 co-utilizes galactose and glucose. *Biotechnol Biofuels* **2019**, *12*, 295.

(14) Banerjee, D.; Eng, T.; Lau, A. K.; Sasaki, Y.; Wang, B.; Chen, Y.; Prahl, J.-P.; Singan, V. R.; Herbert, R. A.; Liu, Y.; et al. Genome-scale metabolic rewiring improves titers rates and yields of the non-native product indigoidine at scale. *Nat. Commun.* **2020**, *11*, 5385.

(15) Kang, C. W.; Lim, H. G.; Yang, J.; Noh, M. H.; Seo, S. W.; Jung, G. Y. Synthetic auxotrophs for stable and tunable maintenance of plasmid copy number. *Metab. Eng.* **2018**, *48*, 121–128.

(16) Elmore, J. R.; Dexter, G. N.; Salvachúa, D.; O'Brien, M.; Klingeman, D. M.; Gorday, K.; Michener, J. K.; Peterson, D. J.; Beckham, G. T.; Guss, A. M. Engineered Pseudomonas putida simultaneously catabolizes five major components of corn stover lignocellulose: Glucose, xylose, arabinose, p-coumaric acid, and acetic acid. *Metab. Eng.* **2020**, *62*, 62–71.

(17) Sandberg, T. E.; Salazar, M. J.; Weng, L. L.; Palsson, B. O.; Feist, A. M. The emergence of adaptive laboratory evolution as an efficient tool for biological discovery and industrial biotechnology. *Metab. Eng.* **2019**, *56*, 1–16.

(18) LaCroix, R. A.; Palsson, B. O.; Feist, A. M. A model for designing adaptive laboratory evolution experiments. *Appl. Environ. Microbiol.* **2017**, *83*.

(19) Wong, B. G.; Mancuso, C. P.; Kiriakov, S.; Bashor, C. J.; Khalil, A. S. Precise, automated control of conditions for high-throughput growth of yeast and bacteria with eVOLVER. *Nat. Biotechnol.* **2018**, *36*, 614–623.

(20) Mohamed, E. T.; Wang, S.; Lennen, R. M.; Herrgård, M. J.; Simmons, B. A.; Singer, S. W.; Feist, A. M. Generation of a platform strain for ionic liquid tolerance using adaptive laboratory evolution. *Microb. Cell Fact.* **2017**, *16*, 204.

(21) Mohamed, E. T.; Werner, A. Z.; Salvachúa, D.; Singer, C. A.; Szostkiewicz, K.; Rafael Jiménez-Díaz, M.; Eng, T.; Radi, M. S.; Simmons, B. A.; Mukhopadhyay, A.; et al. Adaptive laboratory evolution of Pseudomonas putida KT2440 improves p-coumaric and ferulic acid catabolism and tolerance. *Metab. Eng. Commun.* **2020**, *11*, e00143.

(22) Lim, H. G.; Fong, B.; Alarcon, G.; Magurudeniya, H. D.; Eng, T.; Szubin, R.; Olson, C. A.; Palsson, B. O.; Gladden, J. M.; Simmons, B. A.; et al. Generation of ionic liquid tolerant *Pseudomonas putida* KT2440 strains *via* adaptive laboratory evolution. *Green Chem.* **2020**, *22*, 5677–5690.

(23) Nguyen-Vo, T. P.; Liang, Y.; Sankaranarayanan, M.; Seol, E.; Chun, A. Y.; Ashok, S.; Chauhan, A. S.; Kim, J. R.; Park, S. Development of 3-hydroxypropionic-acid-tolerant strain of Escherichia coli W and role of minor global regulator yieP. *Metab. Eng.* **2019**, *53*, 48–58.

(24) Guzmán, G. I.; Sandberg, T. E.; LaCroix, R. A.; Nyerges, Á.; Papp, H.; de Raad, M.; King, Z. A.; Hefner, Y.; Northen, T. R.; Notebaart, R. A.; et al. Enzyme promiscuity shapes adaptation to novel growth substrates. *Mol. Syst. Biol.* **2019**, *15*, e8462.

(25) Mohamed, E. T.; Mundhada, H.; Landberg, J.; Cann, I.; Mackie, R. I.; Nielsen, A. T.; Herrgård, M. J.; Feist, A. M. Generation of an E. coli platform strain for improved sucrose utilization using adaptive laboratory evolution. *Microb. Cell Fact.* **2019**, *18*, 116.

(26) Reider Apel, A.; Ouellet, M.; Szmidt-Middleton, H.; Keasling, J. D.; Mukhopadhyay, A. Evolved hexose transporter enhances xylose uptake and glucose/xylose co-utilization in Saccharomyces cerevisiae. *Sci. Rep.* **2016**, *6*, 19512.

(27) Takahashi, H.; Kumagai, T.; Kitani, K.; Mori, M.; Matoba, Y.; Sugiyama, M. Cloning and characterization of a *Streptomyces* single module type non-ribosomal peptide synthetase catalyzing a blue pigment synthesis. *J. Biol. Chem.* **2007**, *282*, 9073–9081.

(28) Seo, S. W.; Yang, J.-S.; Kim, I.; Yang, J.; Min, B. E.; Kim, S.; Jung, G. Y. Predictive design of mRNA translation initiation region to control prokaryotic translation efficiency. *Metab. Eng.* **2013**, *15*, 67–74.

(29) Deatherage, D. E.; Barrick, J. E. Identification of mutations in laboratory-evolved microbes from next-generation sequencing data using breseq. *Methods Mol. Biol.* **2014**, *1151*, 165–188.

(30) Langmead, B.; Salzberg, S. L. Fast gapped-read alignment with Bowtie 2. *Nat. Methods* **2012**, *9*, 357–359.

(31) Phaneuf, P. V.; Gosting, D.; Palsson, B. O.; Feist, A. M. ALEdb 1.0: a database of mutations from adaptive laboratory evolution experimentation. *Nucleic Acids Res.* **2019**, *47*, D1164–D1171.

(32) Lawrence, M.; Huber, W.; Pagès, H.; Aboyoun, P.; Carlson, M.; Gentleman, R.; Morgan, M. T.; Carey, V. J. Software for computing and annotating genomic ranges. *PLoS Comput. Biol.* **2013**, *9*, e1003118.

(33) Love, M. I.; Huber, W.; Anders, S. Moderated estimation of fold change and' ' dispersion for RNA-seq data with DESeq2. *Genome Biol.* **2014**, *15*, 550.

(34) Yu, D.; Xu, F.; Valiente, J.; Wang, S.; Zhan, J. An indigoidine biosynthetic gene cluster from Streptomyces chromofuscus ATCC 49982 contains an unusual IndB homologue. *J. Ind. Microbiol. Biotechnol.* **2013**, *40*, 159–168.

(35) Sandberg, T. E.; Szubin, R.; Phaneuf, P. V.; Palsson, B. O. Synthetic cross-phyla gene replacement and evolutionary assimilation of major enzymes. *Nat. Ecol. Evol.* **2020**.

(36) Li, G.-M. Mechanisms and functions of DNA mismatch repair. *Cell Res.* **2008**, *18*, 85–98.

(37) Del Castillo, T.; Duque, E.; Ramos, J. L. A set of activators and repressors control peripheral glucose pathways in Pseudomonas putida to yield a common central intermediate. *J. Bacteriol.* **2008**, *190*, 2331–2339.

(38) Swanson, B. L.; Hager, P.; Phibbs, P.; Ochsner, U.; Vasil, M. L.; Hamood, A. N. Characterization of the 2-ketogluconate utilization operon in Pseudomonas aeruginosa PAO1. *Mol. Microbiol.* **2000**, *37*, 561–573.

(39) Udaondo, Z.; Ramos, J.-L.; Segura, A.; Krell, T.; Daddaoua, A. Regulation of carbohydrate degradation pathways in Pseudomonas involves a versatile set of transcriptional regulators. *Microb Biotechnol* **2018**, *11*, 442–454.

(40) Meijnen, J.-P.; de Winde, J. H.; Ruijssenaars, H. J. Metabolic and regulatory rearrangements underlying efficient D-xylose utilization in engineered Pseudomonas putida S12. *J. Biol. Chem.* **2012**, *287*, 14606–14614.

(41) Saravolac, E. G.; Taylor, N. F.; Benz, R.; Hancock, R. E. Purification of glucose-inducible outer membrane protein OprB of Pseudomonas putida and reconstitution of glucose-specific pores. *J. Bacteriol.* **1991**, *173*, 4970–4976.

(42) Bailey, S. F.; Hinz, A.; Kassen, R. Adaptive synonymous mutations in an experimentally evolved Pseudomonas fluorescens population. *Nat. Commun.* **2014**, *5*, 4076.

(43) Dokter, P.; Pronk, J. T.; Schie, B. J.; Dijken, J. P.; Duine, J. A. The in vivo and in vitro substrate specificity of quinoprotein glucose dehydrogenase of *Acinetobacter calcoaceticus* LMD79.41. *FEMS Microbiol. Lett.* **1987**, *43*, 195–200.

(44) Wehrs, M.; Gladden, J. M.; Liu, Y.; Platz, L.; Prahl, J.-P.; Moon, J.; Papa, G.; Sundstrom, E.; Geiselman, G. M.; Tanjore, D.; et al. Sustainable bioproduction of the blue pigment indigoidine: Expanding the range of heterologous products in *R. toruloides* to include non-ribosomal peptides. *Green Chem.* **2019**, *21*, 3394–3406.

(45) Wehrs, M.; Prahl, J.-P.; Moon, J.; Li, Y.; Tanjore, D.; Keasling, J. D.; Pray, T.; Mukhopadhyay, A. Production efficiency of the bacterial non-ribosomal peptide indigoidine relies on the respiratory metabolic state in *S. cerevisiae*. *Microb. Cell Fact.* **2018**, *17*, 193.

(46) Lim, H. G.; Kwak, D. H.; Park, S.; Woo, S.; Yang, J. S.; Kang, C. W.; Kim, B.; Noh, M. H.; Seo, S. W.; Jung, G. Y. *Vibrio* sp. dhg as a platform for the biorefinery of brown macroalgae. *Nat. Commun.* **2019**, *10*, 2486.

(47) Linger, J. G.; Vardon, D. R.; Guarnieri, M. T.; Karp, E. M.; Hunsinger, G. B.; Franden, M. A.; Johnson, C. W.; Chupka, G.; Strathmann, T. J.; Pienkos, P. T.; et al. Lignin valorization through integrated biological funneling and chemical catalysis. *Proc. Natl. Acad. Sci. USA* **2014**, *111*, 12013–12018.

(48) Yaegashi, J.; Kirby, J.; Ito, M.; Sun, J.; Dutta, T.; Mirsiaghi, M.; Sundstrom, E. R.; Rodriguez, A.; Baidoo, E.; Tanjore, D.; et al. Rhodosporidium toruloides: a new platform organism for conversion of lignocellulose into terpene biofuels and bioproducts. *Biotechnol Biofuels* **2017**, *10*, 241.

(49) Wargacki, A. J.; Leonard, E.; Win, M. N.; Regitsky, D. D.; Santos, C. N. S.; Kim, P. B.; Cooper, S. R.; Raisner, R. M.; Herman, A.; Sivitz, A. B.; et al. An engineered microbial platform for direct biofuel production from brown macroalgae. *Science* **2012**, *335*, 308–313.

(50) Antonovsky, N.; Gleizer, S.; Noor, E.; Zohar, Y.; Herz, E.; Barenholz, U.; Zelcbuch, L.; Amram, S.; Wides, A.; Tepper, N.; et al. Sugar Synthesis from CO2 in *Escherichia coli*. *Cell* **2016**, *166*, 115–125.

(51) Enquist-Newman, M.; Faust, A. M. E.; Bravo, D. D.; Santos, C. N. S.; Raisner, R. M.; Hanel, A.; Sarvabhowman, P.; Le, C.; Regitsky, D. D.; Cooper, S. R.; et al. Efficient ethanol production from brown macroalgae sugars by a synthetic yeast platform. *Nature* **2014**, *505*, 239–243.

(52) Sandberg, T. E.; Lloyd, C. J.; Palsson, B. O.; Feist, A. M. Laboratory evolution to alternating substrate environments yields distinct phenotypic and genetic adaptive strategies. *Appl. Environ. Microbiol.* **2017**, *83*.

(53) Sharma, V.; Kumar, V.; Archana, G.; Kumar, G. N. Substrate specificity of glucose dehydrogenase (GDH) of Enterobacter asburiae PSI3 and rock phosphate solubilization with GDH substrates as C sources. *Can. J. Microbiol.* **2005**, *51*, 477–482.

(54) Igarashi, S.; Hirokawa, T.; Sode, K. Engineering PQQ glucose dehydrogenase with improved substrate specificity. Site-directed mutagenesis studies on the active center of PQQ glucose dehydrogenase. *Biomol Eng* **2004**, *21*, 81–89.

(55) Wang, L.; York, S. W.; Ingram, L. O.; Shanmugam, K. T. Simultaneous fermentation of biomass-derived sugars to ethanol by a co-culture of an engineered Escherichia coli and Saccharomyces cerevisiae. *Bioresour. Technol.* **2019**, *273*, 269–276.

(56) Zhang, H.; Pereira, B.; Li, Z.; Stephanopoulos, G. Engineering *Escherichia coli* coculture systems for the production of biochemical products. *Proc. Natl. Acad. Sci. USA* **2015**, *112*, 8266–8271.

(57) Quan, S.; Ray, J. C. J.; Kwota, Z.; Duong, T.; Balázsi, G.; Cooper, T. F.; Monds, R. D. Adaptive evolution of the lactose utilization network in experimentally evolved populations of Escherichia coli. *PLoS Genet.* **2012**, *8*, e1002444.

(58) Lee, D.-H.; Feist, A. M.; Barrett, C. L.; Palsson, B. Ø. Cumulative number of cell divisions as a meaningful timescale for adaptive laboratory evolution of Escherichia coli. *PLoS One* **2011**, *6*, e26172.

675 **Table**

676 **Table 1. Commonly mutated genes and regions in evolved strains**

Region	Gene product	Frequency (total samples)	Number of unique mutations
P. putida xylD		*n* = 11	
ptxS	Ketogluconate utilization operon repressor	100% (ALE1-4)	5
kguT	2-Ketogluconate transporter	82% (ALE1-4)	9
gacS	Sensor protein	36% (ALE2 and ALE3)	3
ftsH	Integral membrane ATP-dependent zinc metallopeptidase	27% (ALE2 and ALE4)	3
PP_4173	Two-component system sensor histidine kinase/response regulator	27% (ALE1 and ALE2)	3
galP-I /PP_1174	Porin-like protein/hypothetical protein	18% (ALE2 and ALE4)	2
P. putida galETKM		*n* = 12	
gtsABCD	Mannose/glucose ABC transporter	66% (ALE5, ALE6, ALE8)	7
oprB-I/*yeaD*	Carbohydrate-selective porin-I/glucose-6-phosphate 1-epimerase	58% (ALE5, ALE6, ALE8)	4
oprB-II	Carbohydrate-selective porin-II	17% (ALE5 and ALE8)	1

677

678

679

Figure caption

Figure 1. Adaptive Laboratory Evolution (ALE) strategies for improving xylose and galactose utilization

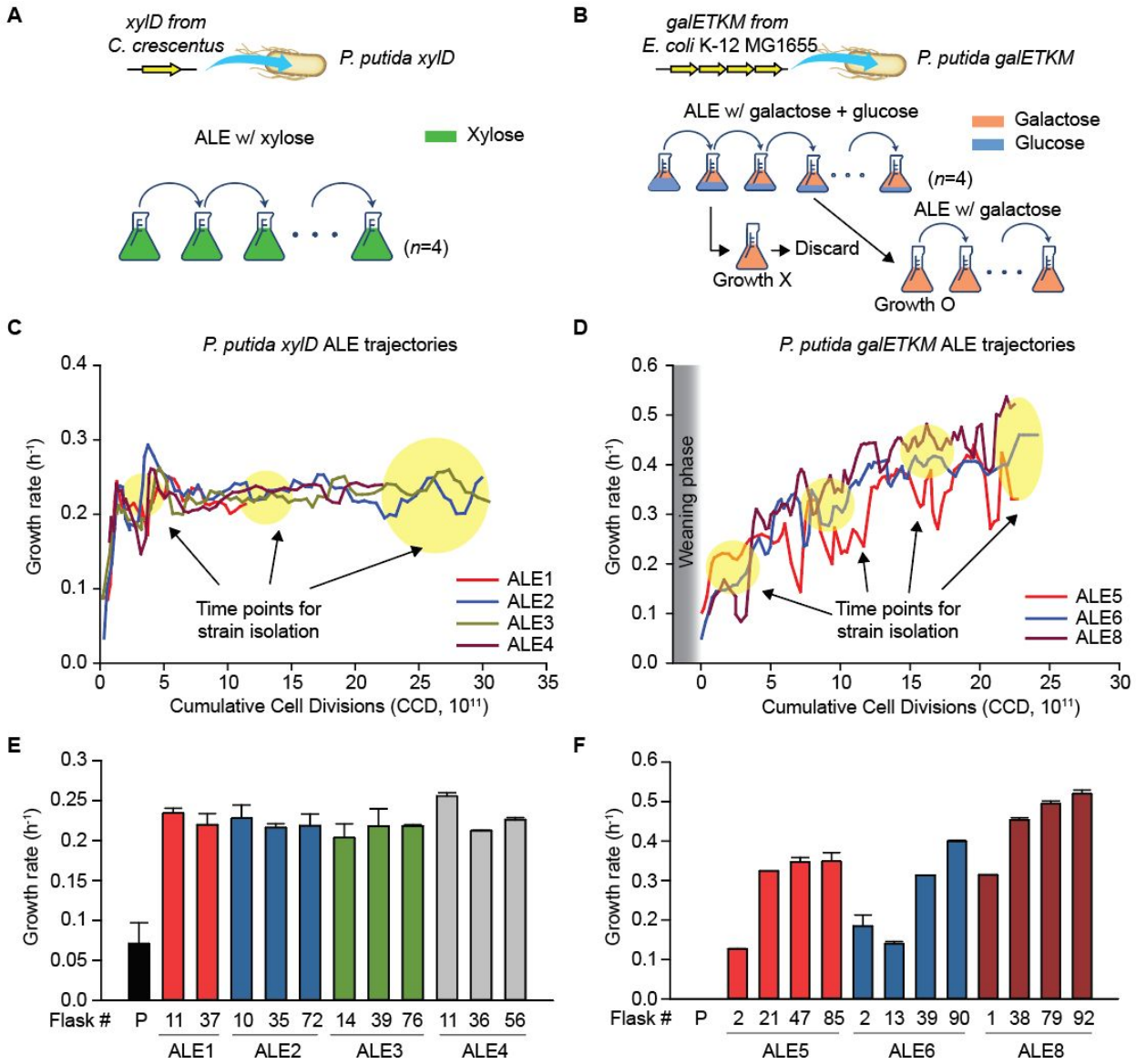

(A and B) The ALE strategies to evolve the *P. putida xylD* and *P. putida galETKM* strains. Growth trajectories of **(C)** ALE1-4 and **(D)** ALE5, ALE6, and ALE8 with the *xylD* and *galETKM* strains, respectively. The *x*-axis and *y*-axis indicate Cumulative Cell Divisions (CCD)[61] and the maximum specific growth rate (h^{-1}). CCD for the galactose ALE experiments were calculated from the first

flask which displayed an observable growth rate solely on galactose minimal media. Comparisons of the maximum specific growth rates (h^{-1}) of isolated clones from different evolutionary timepoints of **(E)** ALE1-4 and **(F)** ALE5, ALE6, and ALE8. Cell cultures were conducted in biological duplicates and error bars indicate the minimum and maximum values.

Figure 2. Growth profiles of the wildtype KT2440 and evolved isolates

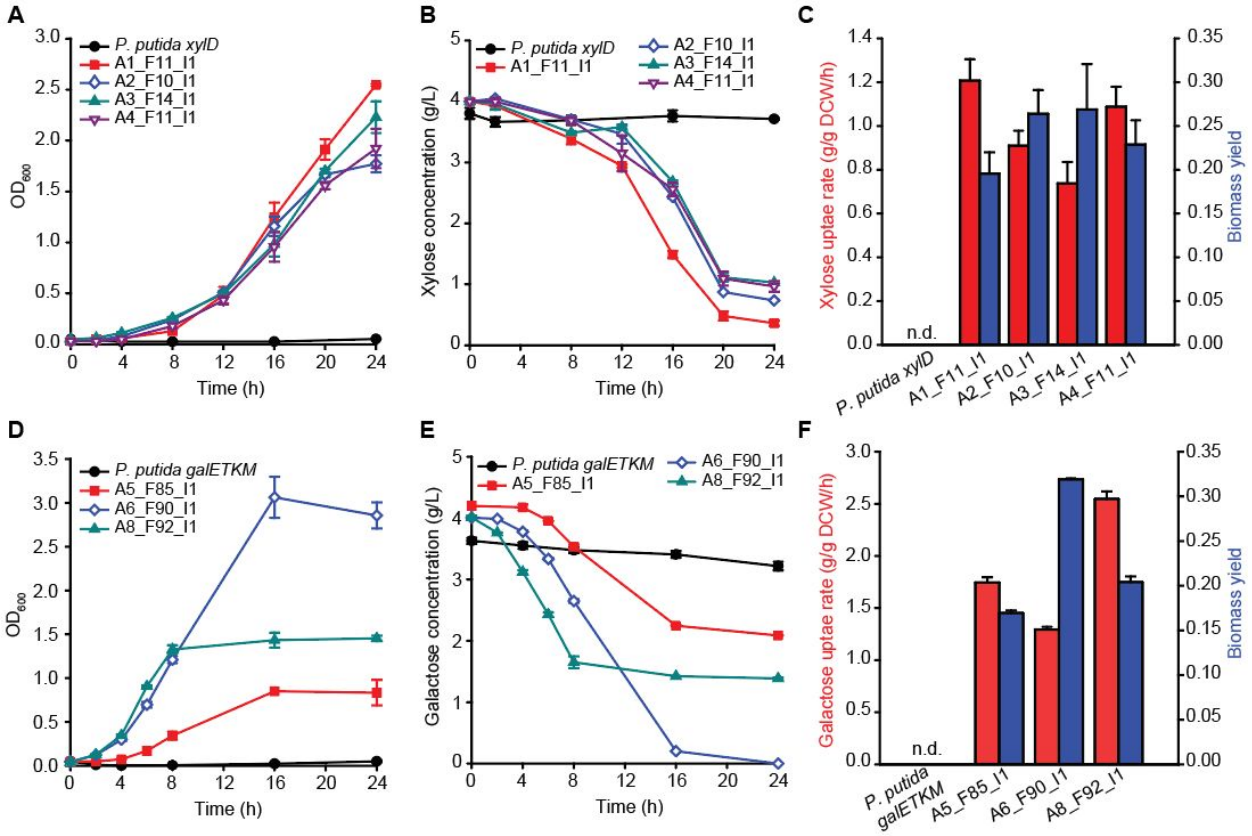

(A) Growth, (B) xylose consumption, (C) xylose uptake rates and biomass yields of the *P. putida xylD* strain and evolved isolates in the xylose minimal medium during a 24 h cultivation. (D) Growth, (E) galactose consumption, (F) galactose uptake rates and biomass yields of the *P. putida galETKM* strain and evolved isolates on galactose in the galactose minimal medium during a 24 h cultivation. (A, B, D, E) *x*-axis indicates time (h) and left *y*-axis indicates (A and D) OD_{600} or (B and E) sugar concentration (g/L). (C and F) left and right y-axis indicates sugar consumption rate during the exponential growth phase and biomass yield, respectively. The cultures were conducted with three biological replicates (n=3) and error bars indicate the standard deviations.

Figure 3. Genomic and transcriptomic analysis of evolved isolates

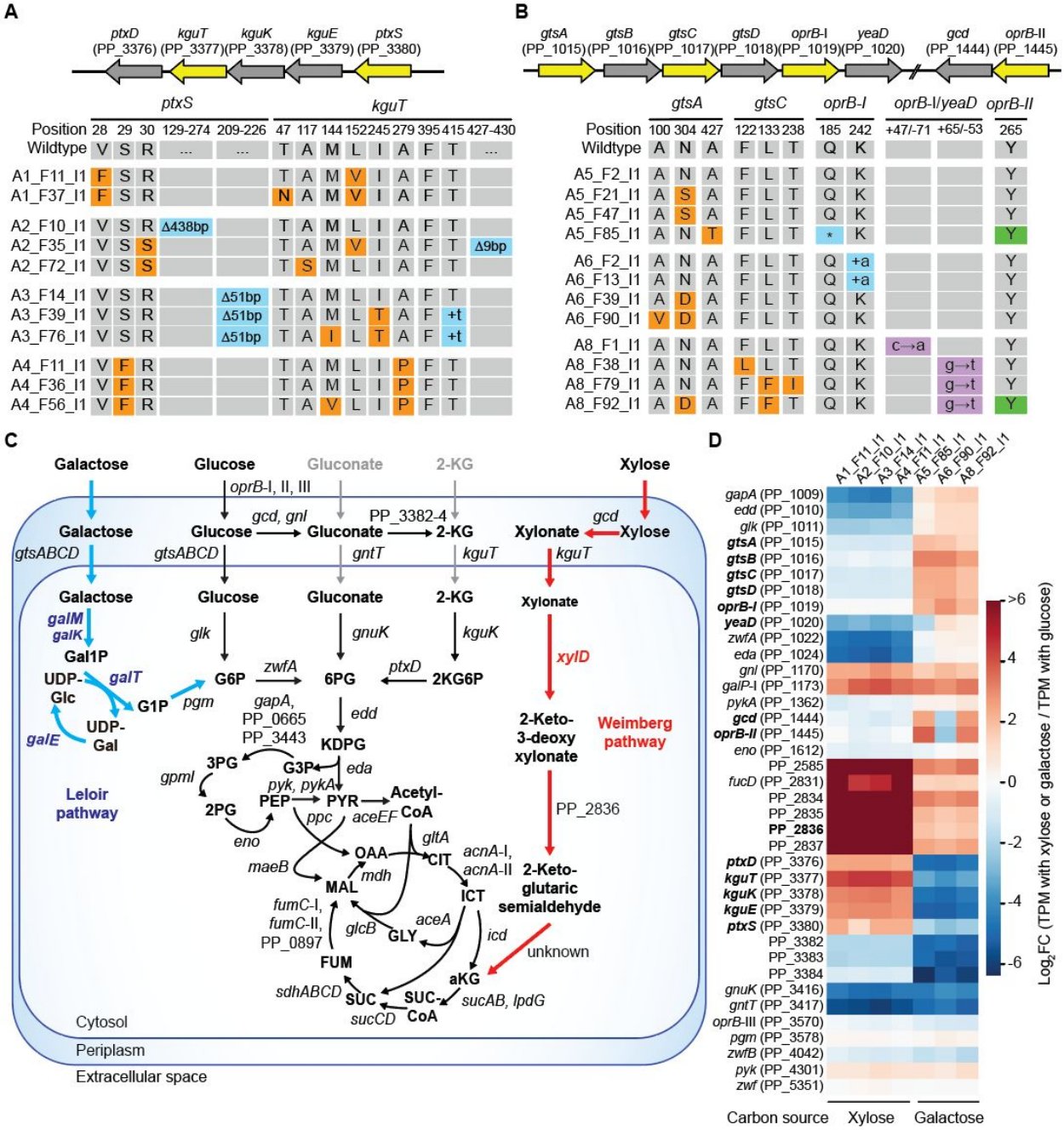

(A and B) Identified mutations in **(A)** the *ptxS-kguEKT-ptxD* region of evolved *P. putida xylD* clones and **(B)** the *gtsA-gtsBCD-oprB*-I-*yeaD* and *oprB*-II-*gcd* regions of evolved *P. putida galETKM* clones. **(A and B)** Uppercase and lowercase letters indicate amino acids and nucleobases, respectively. * indicates the early termination mutation. Arrow sizes do not represent gene lengths.

Colors: blue, amino acid deletions, frame shift mutations, early termination mutations; green, synonymous mutations; purple, single nucleotide mutations; orange, single amino acid changes. **(C)** Central carbon metabolism of KT2440 with the heterologous xylose and galactose utilization genes. Red and blue arrows indicate the Weimberg and Leloir pathways, respectively. Heterologous genes were colored in red or blue. Abbreviations: 2-KG, 2-ketogluconate; G6P, glucose-6-phosphate (P); 6PG, 6-phosphogluconate; 2KG6P, 2-ketogluconate-6-P; Gal1P, galactose-1-P; UDP-Glc, uridine diphosphate-glucose; UDP-Gal, uridine diphosphate galactose; G1P, glucose-1-P; KDPG, 2-dehydro-3-deoxy-phosphogluconate; PYR, pyruvate; G3P, glyceraldehyde-3-P; 3PG, glycerate-3-P; 2PG, 2-phosphoglycerate; PEP, phosphoenolpyruvate; acetyl-CoA, acetyl coenzyme A (CoA), CIT, citrate; ICT, isocitrate; αKG, α-ketoglutarate; SUC-CoA, succinyl-CoA; SUC, succinate; FUM, fumarate; MAL, malate; OAA, oxaloacetate; GLY, glyoxylate. Genes in bold are involved in xylose or galactose utilization or close to mutated genes. **(D)** Log_2 Transcripts Per Million (TPM) fold changes of genes related to sugar catabolism. Actual values were provided in Supplementary Data 3.

Figure 4. Validation of xylose and galactose metabolism in evolved strains

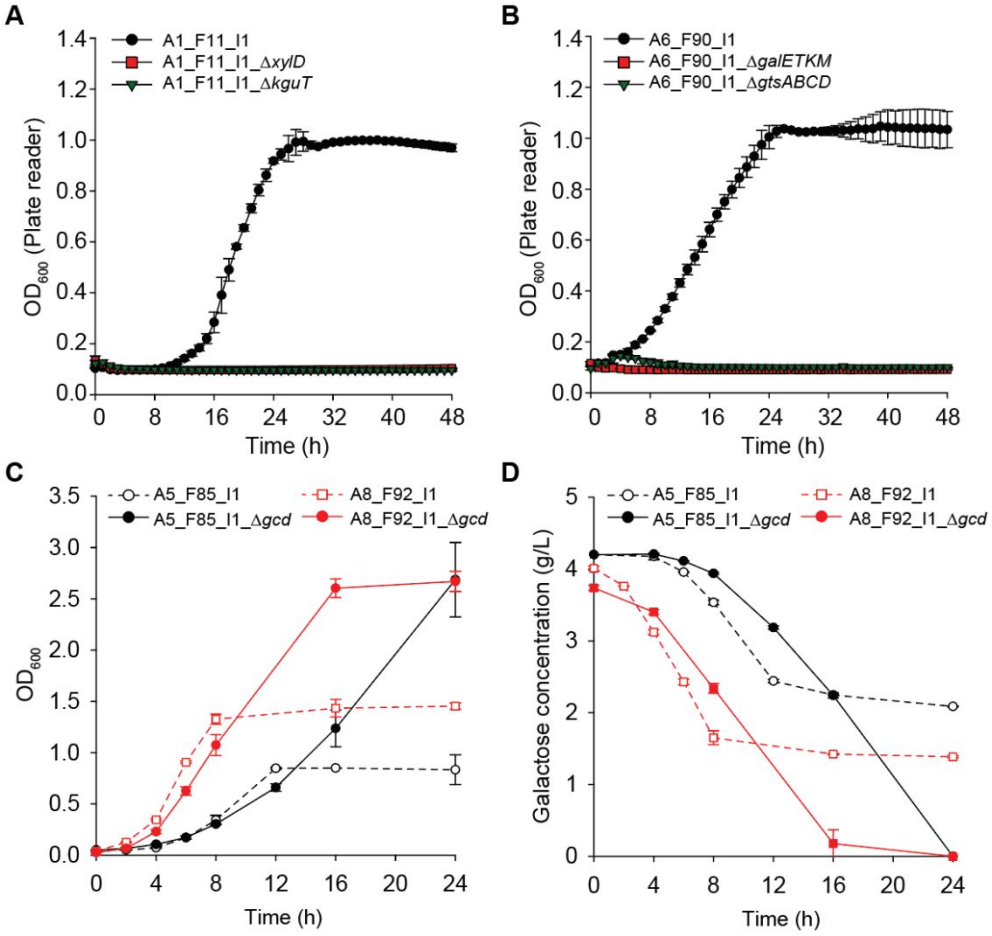

(A and B) Growth profiles of the **(A)** A1_F11_I1 (black circle), A1_F11_I1_Δ*xylD* (red square), and A1_F11_I1_Δ*kguT* (green down triangle) strains in the xylose minimal medium and **(B)** A6_F90_I1 (black circle), A6_F90_I1_Δ*galETKM* (red square), and A6_F90_I1_Δ*gtsABCD* (green down triangle) strains in the galactose minimal medium. These strains were cultivated using a microtiter plate reader. Growth **(C)** and sugar consumption profiles **(D)** of A5_F85_I1 (black open circle), A5_F85_I1_Δ*gcd* (black closed circle), A8_F92_I1 (red open square), A8_F92_I1_Δ*gcd* (red closed square) strains. **(A-D)** *x*-axis indicates time (h). *y*-axis indicates **(A-C)** OD_{600} or **(D)** galactose concentration (g/L). The cultures were conducted with three biological replicates (n=3) and error bars indicate the standard deviations.

Figure 5. Indigoidine production from xylose and galactose by using evolved strains as hosts

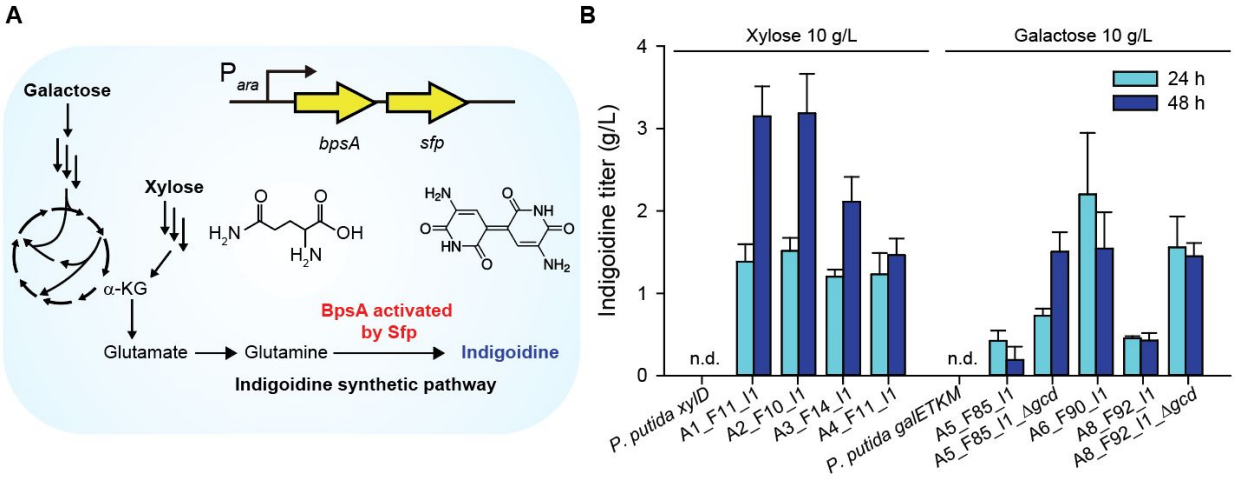

(A) The indigoidine production pathway engineered into *P. putida* strains. Indigoidine can be produced by heterologous expression of *bpsA* from *S. lavendulae* and *sfp* from *B. subtilis* for conversion of glutamine. These genes were expressed under the arabinose inducible promoter (P_{ara}). **(B)** Comparison of the indigoidine titers (g/L) of the initial engineered strains (not detected, n.d.), evolved isolates, and two evolved isolates with a *gcd* deletion after 24 h (light blue) and 48 h (dark blue) cultivation. The *bpsA* and *sgfp* expression cassette was integrated into the chromosome of each host strain. Four biological replicates (n=4) were performed, and error bars indicate the standard deviations.